

**INVESTIGATION OF STRESS DISTRIBUTION IN
OPTIMIZED CONCRETE SHELL STRUCTURES
UNDER STATIC LOADING**



FINAL YEAR PROJECT UG 2016

By

Leader - 175599 Abdul Hayee

Member 1 - 195663 Ali Abdul Moiz Waseem

Member 2 - 199363 Muhammad Saad ur Rehman

Member 3 - 177058 M. Hasnain Ahmad

NUST Institute of Civil Engineering
School of Civil and Environmental Engineering
National University of Sciences and Technology, Islamabad, Pakistan

2020

This is to certify that the

Final Year Project Titled

**INVESTIGATION OF STRESS DISTRIBUTION IN
OPTIMIZED CONCRETE SHELL STRUCTURES
UNDER STATIC LOADING**

submitted by

Leader - 175599 Abdul Hayee

Member 1 - 195663 Ali Abdul Moiz Waseem

Member 2 - 199363 Muhammad Saad ur Rehman

Member 3 - 177058 M. Hasnain Ahmad

has been accepted towards the requirements
for the undergraduate degree

in

CIVIL ENGINEERING

Dr. Azam Khan
Assistant Professor
NUST Institute of Civil Engineering
School of Civil and Environmental Engineering
National University of Sciences and Technology, Islamabad, Pakistan

ABSTRACT

This is a study to investigate the stress distribution in optimized concrete shell structures and presenting them as a viable and economical structural option.

The group began the study by building their understanding of Finite Element Method and Linear Optimization to familiarize themselves with the basics of advanced structural analysis and optimization. This initial understanding paved the way for a much comfortable experience in using ABAQUS/CAE for analysis and optimization works. The group then studied about the prevalence of concrete shells in Pakistan and found that benefits of concrete shells are not being utilized in Pakistan and hence it justified the need to research on the viability of concrete shells as a structural option.

From literature review, it was realized that it is yet to be extensively studied to reach a distribution of stresses in the shells' thickness which is as uniform as possible to have the shells free of bending. For this reason, optimization of shell structures was further studied. optimization techniques are applied to find variation in designs of concrete shells complying with the design conditions and to study the effect of optimization on the stress distribution in shell structures. To achieve this task, optimization techniques are applied to a basic shell structures to study its effects on the original shape and design. It is also explored how shells are more economical and stable than traditional frame structures.

The results of stresses from a basic optimized shell were compared to those obtained from a frame building having equal material used and same load values and combinations applied. It was seen that the optimized shell was more efficient in terms of resisting the loads and generated lesser values of maximum stresses.

Keywords: Shells, Concrete, Optimization, Stress Distribution

DEDICATION

To our beloved parents who gave us strength, and who continually provide us with their moral, spiritual, emotional, and financial support.

To our teachers and mentors who enabled us and guided us to carry out this study.

To our friends and classmates who have been good companions in our undergraduate journey.

To those researchers who have worked on this topic before us and formed the grounds on which we could further the quest of knowledge.

And to the heroes who are fighting for the betterment of society and who are working day and night on the frontlines to keep us all safe and healthy in the face of an unprecedented pandemic of such gargantuan scale.

ACKNOWLEDGMENTS

Foremost, we would like to express our sincere gratitude to our advisor Dr. Azam Khan for his continued support and guidance throughout our research, for his patience, enthusiasm, and immense knowledge and abilities. His guidance helped us in finalizing a topic for our research, doing the prerequisite study and literature review, forming the research objectives and methodology, and seeing everything through even in these challenging times when the world is grappling with an unprecedented pandemic.

Besides our advisor, we would like to extend our sincerest gratitude to Dr. Usman Hanif, Lecturer Samiullah Khan Bangash, Lecturer Muhammad Asim Ayaz - the faculty members at NUST Institute of Civil Engineering who provided key valuable insights into how we can better shape our research.

Lastly, we would like to acknowledge the NUST Project Management Office for providing us with drawings of NUST's Jinnah Auditorium whose contribution and requirement was fundamental to our research.

TABLE OF CONTENTS

LIST OF TABLES	viii
LIST OF FIGURES	ix
NOMENCLATURE	xi
CHAPTER 1	1
1.1 General	1
1.2 Background	2
1.3 Introduction to Shell Structures	2
1.4 Scope	3
CHAPTER 2	4
2.1 Introduction	4
2.2 Previous Work	4
2.3 Conclusion	5
CHAPTER 3	6
3.1 Overview	6
3.2 Stress Distribution of an Optimized Shell	6
3.2.1 Properties Definition	7
3.2.2 Assembly	8
3.2.3 Loading	8
3.2.4 Meshing	8
3.2.5 Job Execution	9
3.2.6 Load Combinations	10
3.2.7 Further Iterations	13
3.3 Comparison with an Equivalent Frame Structure	14
3.3.1 Code Selection	14
3.3.2 Materials Definition	15
3.3.3 Members Definition	16
3.3.4 Grid Layout and Members Placement	17

3.3.5 Check on Model.....	21
3.3.6 Applied Loads and Load Combinations	21
3.3.7 Meshing and Analysis	22
3.3.8 Stress Distribution and Deformations.....	22
3.4 Provision for Stability of Shell Formwork.....	24
 CHAPTER 4	 27
4.1 Parameters from ETABS.....	27
4.2 Parameters from ABAQUS.....	27
4.3 Comments.....	28
 CHAPTER 5	 29
 CHAPTER 6	 30
 APPENDICES	 31
 REFERENCES	 34

LIST OF TABLES

Table 1: Concrete Damaged Plasticity Module	12
Table 2: Concrete Strengths.....	15
Table 3: Load Combinations	23
Table 4: Parameters for ETABS Model	28
Table 5: Parameters for ABAQUS Model	28

LIST OF FIGURES

Figure 1: Types of Shell Structures	3
Figure 2: Shell part.....	6
Figure 3: Shell Section Definition Menu	7
Figure 4: Independent Instance	8
Figure 5: Meshed Part.....	9
Figure 6: Stress Distribution	10
Figure 7: Translation Distribution	10
Figure 8: Stress Distribution	11
Figure 9: Translation Distribution	11
Figure 10: Stress Distribution	12
Figure 11: Translation Distribution	13
Figure 12: Stress Distribution	13
Figure 13: Translation Distribution	14
Figure 14: Code Selection.....	15
Figure 15: Circular Grid.....	17
Figure 16: Circular & Rectangular Grids in Combination.....	18
Figure 17: Columns & Shear Walls Placed on Grid.....	19
Figure 18: Beams Placed	20
Figure 19: Completed Frame Structure.....	21
Figure 20: Deformed Structure	23
Figure 21: Stress Distribution	23
Figure 22: Strengthened Temporary Work frame (Type A).....	24

Figure 23: Non-strengthened Temporary Work Frame (Type B).....	25
Figure 24: Arrangement of Type-A rane in a Dome Temporary Works	26
Figure 25: Maximum story displacements of ETABS model.....	32
Figure 26: Different types of joints used in steel tube temporary works.....	33

NOMENCLATURE

<i>in</i>	inches
<i>lb</i>	pounds
<i>psi</i>	pounds per square inch
<i>psf</i>	pounds per square feet
<i>lb/in³</i>	pounds per cubic inch
<i>cft</i>	cubic foot

INTRODUCTION

1.1 General

This thesis deals with the study of stress distribution and optimization of shell structures and aims at presenting thin concrete shells as a relevant and valuable structural solution.

In the design of any structure, the designers always aim to achieve economy by minimizing costs within the constraints of structural, aesthetic, safety, and functional requirements. The designers and architects thus endeavor to find new construction materials which are cheaper and stronger, or with the available materials, try to evolve new forms that resist the loads more efficiently than when the structure is designed in a conventional form. Shell structures are an example of one such form which fulfill both the architects' desire of innovative and aesthetic designs and the engineers' need for a stable and sound structural form.

Optimization of a structure enables both the architect and the engineer to collaborate on a given project right from the start by giving both the parties an improved shape based on their given design. Thus, an integrated design approach comes into play in the form of an iterative cycle of design and optimization.

In Pakistan, most of the design work is limited to being done through building and design codes which leaves a lot of room for improvement in the efficiency of the design. Optimization is a technique which fills up that room. This unique approach helps in saving time to produce a uniquely tailored solution for a given project.

Considering this, the thesis looks to explore the use of optimized shell structures and presenting them as a viable structural option, thus advancing the knowledge on shell structures in Pakistan's academic sphere.

1.2 Background

Triangular form of distribution of stresses through a cross section is uneconomical since the maximum stress occurs on the outer fibers. This is particularly true for concrete, whose resistance to tension is small as compared to compression, and the resistance capacity of the cross section is drained as soon as the minimum value is reached.

Shells, compared other types of structures, have a structural behavior that is characterized by higher mechanical efficiency. Concrete shells depend on their shape and configuration, and not on their mass, for stability. If proper designs are carried out, shells can support high loads and allow one to cover important spaces using little material and thickness. Moreover, shells present an attractive lightness and elegance from an aesthetic point of view.

The structural behavior of shells is developed principally due to their form. It is of interest to find that if small alterations in their geometry without amending their initial aesthetic configuration too much can still comply with the design conditions. These modifications would improve that mechanical behavior still further. It could be tried, for example, to reach a distribution of stresses in the thickness which is as uniform as possible, and this would imply to have shells free of bending or with some acceptable bending values [1].

Among different methods used in shape-finding of concrete shells, optimization techniques represent an effective means to achieve this purpose. These techniques allow to obtain alternative geometric forms of shells and improve their mechanical behavior, conforming with the design conditions in an optimum way.

1.3 Introduction to Shell Structures

Shell structures are considered one of the most efficient known structural forms. They are a perfect example of achieving strength through form as opposed to strength through mass. Reinforced concrete shells have many applications in several civil engineering fields and may be used at roofs, water tanks, pressure vessels, tunnels, cooling towers, canals, foundations, and dams, among others.

Shells have a curved plate structure having small thickness as compared to other dimensions. Shells carry loads mainly in direct compression or tension, rather than in bending or shear and possess strength and rigidity due to their thin curved form. Shells were largely forgotten after 17th century but their recent need has been stimulated by the newly developed reinforced concrete and the demand to cover long-spans.

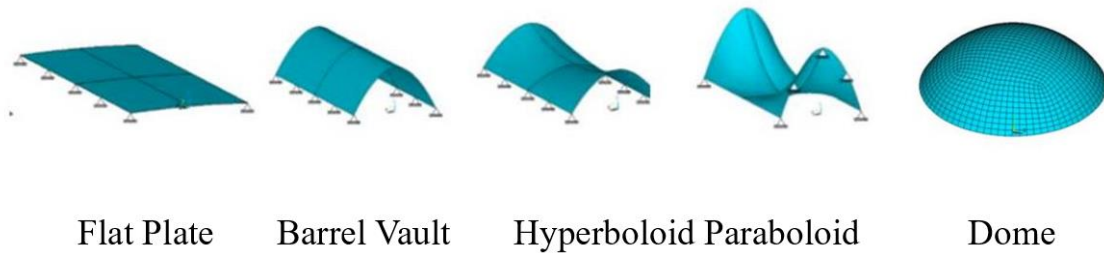


Figure 1 - Types of Shell Structures

On the advantages of concrete shells, they have an efficient resistant mechanism through their inherently strong structures. Concrete, as a material, can be easily cast into curves. Shells provide aesthetics, economy, long unobstructed interiors, and small deformations all in a single package. Moreover, shells provide excellent support against rain and snow loads.

1.4 Scope

In this thesis, optimization techniques are applied to find variation in designs of concrete shells complying with the design conditions and to study the effect of optimization on the stress distribution in shell structures. To achieve this task, optimization techniques are applied to a basic shell structures to study its effects on the original shape and design. It is also explored how shells are more economical and stable than traditional frame structures.

ABAQUS/CAE was chosen for the analysis and optimization of the shell structure. It was realized that the other software options available had outdated interfaces or just were not suitable to the needs of the study.

LITERATURE REVIEW

2.1 Introduction

This chapter brings an insight into what previous work has been done on the optimization of shell structures, what gaps are there in the current knowledge of optimization in relation to shell structures, and what work is done in this study to cover some of those gaps.

Shells have their unique behavior due to their form. Therefore, it is of interest to find that if small alterations in their geometry without amending their initial aesthetic configuration too much can still comply with the design conditions. These modifications would improve that mechanical behavior still further.

Many recent studies have been done to study what kind of and to what extent these modifications can be done. To reach a balance between such modifications and the requirements of economy, functionality and design, optimization has been studied. Among different techniques used for such modifications [2], optimization techniques represent an effective means to obtain optimum designs against given design conditions.

While there has been much research on optimization techniques and their results, few researchers have taken the effect of optimization on stress distribution of shells into consideration. Therefore, a gap was identified, and it was realized that further studies need to be done on the effect of optimization on the stress distribution of shells. Therefore, a gap was identified, and it was realized that further studies need to be done on the effect of optimization on the stress distribution of shells.

2.2 Previous Work

As described above, the problem of optimization of shells has been of importance to both researchers and structural engineers in the past. Many authors had developed algorithms to optimize the shape and size of shell structures. Shape and size optimization of shell

structures using finite element method was examined by Bletzinger and Ramm [2], Rao and Hinton [3], Afonso and Hinton [4], Ghasemi [5] and Lee [6]. Hinton et al [7] and Rao et al [8] also carried out shape and size optimization of prismatic shell structures using the finite strip method. These studies used the analytical procedures related to finite elements to carry out optimizations in shape functions of shell structures.

Shimoda and Ikeya [9] proposed a non-parametric free-form optimization method of shell structures with curvature constraint. Similar work was done by Fujita and Ohsaki [10]. The studies did not specify any parameters for the optimization.

Gotsis [11] did a study on structural optimization of thin shell structures that are subjected to stress and displacement constraints. This study provided a good understanding of the basic problem at hand and gave an insight into our own work.

2.3 Conclusion

These works give the researcher a good idea on how a good deal of work has been done on the optimization and form finding of shell structures. But its effect on the stress distribution of shells has been largely forgone. This gap is the previous research paved the way for our study.

METHODOLOGY

3.1 Overview

The core focus of this project was to propose a semi-spherical hollow dome that was not only easy to construct but at the same time served as an optimized solution for moving away from the undesired and ubiquitous block-shaped reinforced concrete frame structures that exist in Pakistan. For simplicity and to establish grounds for further research, this study limited its scope to proposing an alternative dome to large block shaped structures prevalent in Pakistan that are used to cover long spans.

3.2 Stress Distribution of an Optimized Shell

This portion of work was mainly undertaken on ABAQUS/CAE. On ABAQUS, for an equivalent area of 22392.595 square feet, a 6” thick dome was modeled whose radius was calculated to be 89.94 feet. However, for coherency of units throughout the model, the radius was computed as 1079.28 inches and the model was generated as shown in Figure 2.

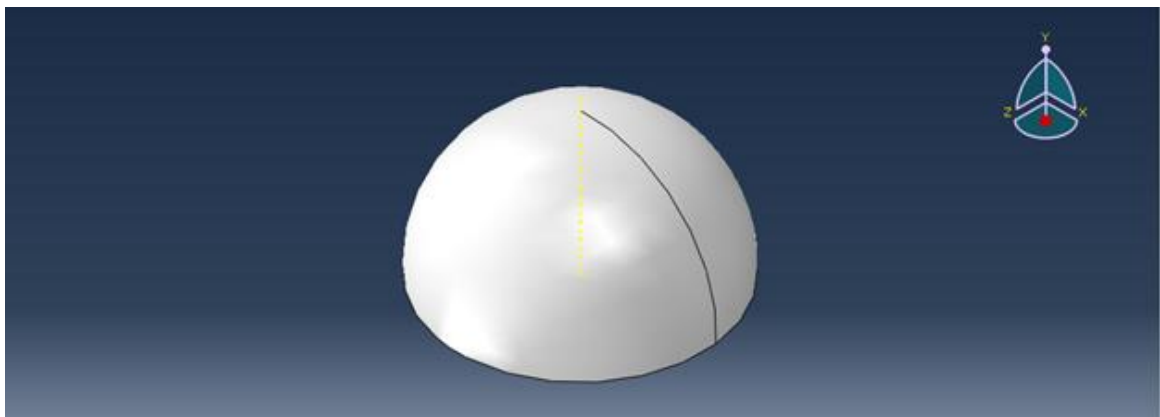


Figure 2 - Shell part

3.2.1 Properties Definition

The next task was to define the properties of the concrete to be used in the model. Considering the ensuing pandemic and the subsequent lockdown of all educational institutes and laboratories, a paper [12] by Jankowiak T. and Lodygowski T. was utilized for these reasons and another which will be expounded upon later.

In reference to the paper [12], the density of the concrete was taken as 0.0868 lb/in^3 , the strength, Young's elastic modulus, and Poisson's ratio were defined as 2500 psi, 2857243 psi and 0.15, respectively.

Next, the section of the shell was defined by selecting the concrete with the properties assigned and the designated thickness. This step was followed by assigning the design part with this section.

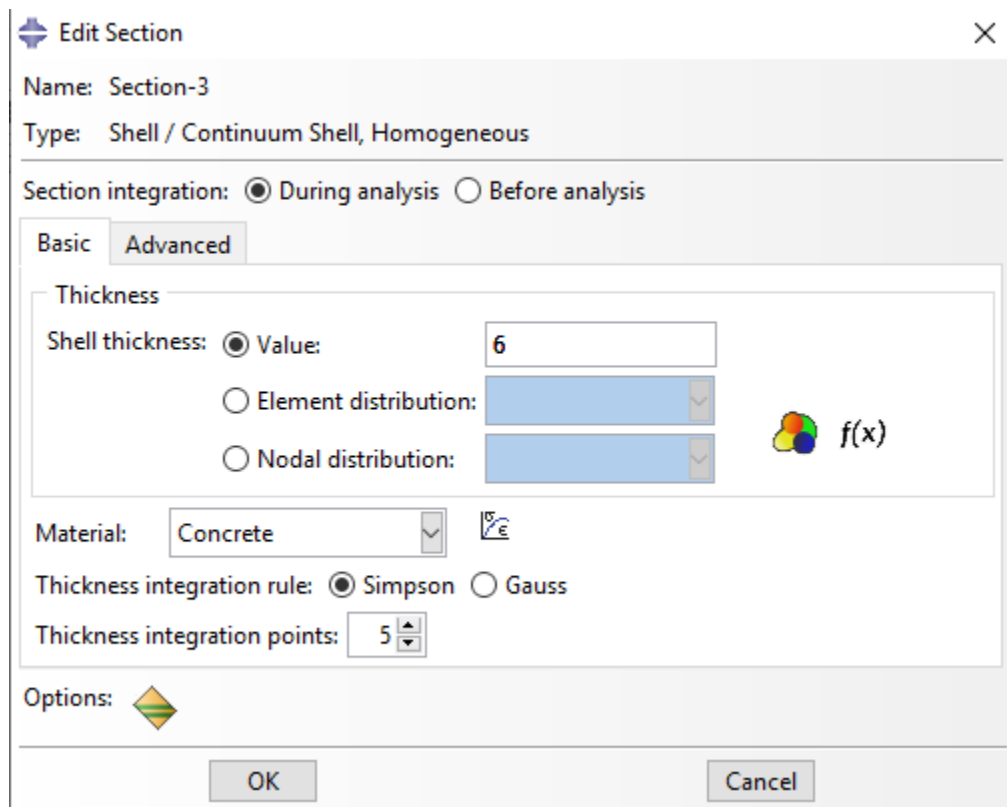


Figure 3 - Shell Section Definition Menu

3.2.2 Assembly

In the next step, the “Assembly” module was used, and our designated part was selected as an independent instance, so that the meshing occurs without any reliance on the individual part’s geometry. The instance is showed in Figure 4.

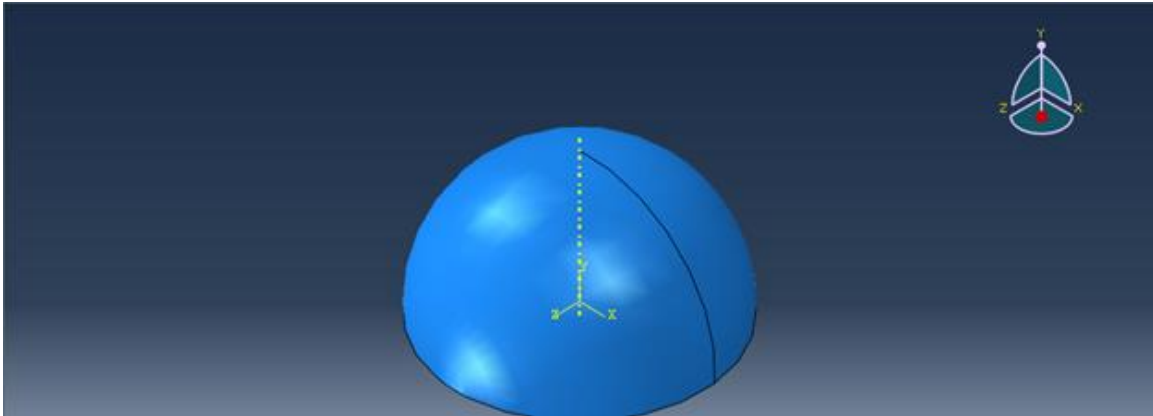


Figure 4 - Independent Instance

3.2.3 Loading

The loading step was then created and selected under the category of “Static; General”, to initially test that if our proposed model can sustain itself under the influence of its own self-weight. For this purpose, a gravity load was created in the “Load” module where the gravity of acceleration was specified. Simultaneously, the boundary conditions are selected as fixed or “ENCASTRE” at the base of the shell structure.

3.2.4 Meshing

In the mesh module, based on the limitation of processing power of the computers being utilized, the finest mesh elements had lengths of 35 inches which generated 12906 elements across the entire shell. The complexity of the structure required that Bottom-up triangular elements be used as it uses the part’s geometry as a guideline for the outer bounds of the

mesh, but the mesh does not conform to geometry. This method of meshing provides the user with the most control over the mesh because the user has the autonomy to select not only the method, but the parameters that define the mesh. The part was meshed to generate the model as shown in Figure 5.

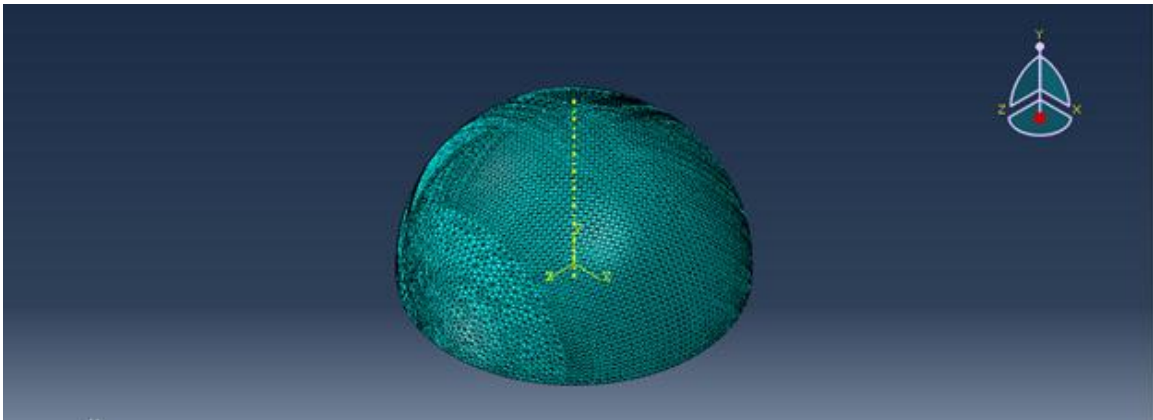


Figure 5 - Meshed Part

3.2.5 Job Execution

To run an analysis on our proposed model, the “Job” module was selected to create a job file for running the stress analysis under the Shell structure self-weight. Once the job file completed the execution, the maximum principal stresses and the maximum deflections were assessed to ascertain if the structure failed or not. The maximum stress, whose location is identified in Figure 6, was computed to be 2233 psi and the maximum displacement, whose location is identified in Figure 7, was computed to be 1.964 inches. It was, therefore, concluded that the structure is stable under its self-weight. For the sake of practicality, in the next phase, a roof load (L_r) of 20 psf, applied as a body force of 0.02327 lb/in^3 in the negative Y-direction, and a load combination from the ASCE7-10 Manual of $1.2D+1.6L_r$ are utilized.

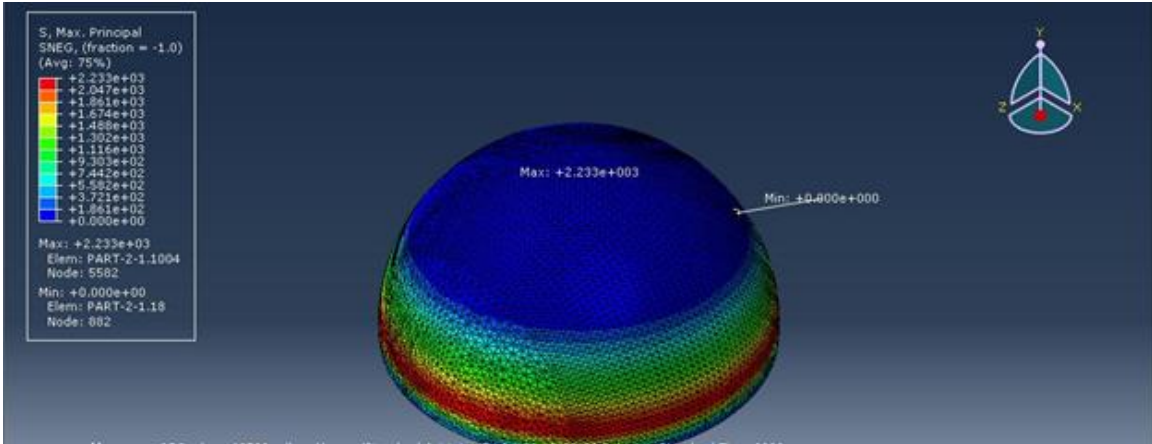


Figure 6 - Stress Distribution

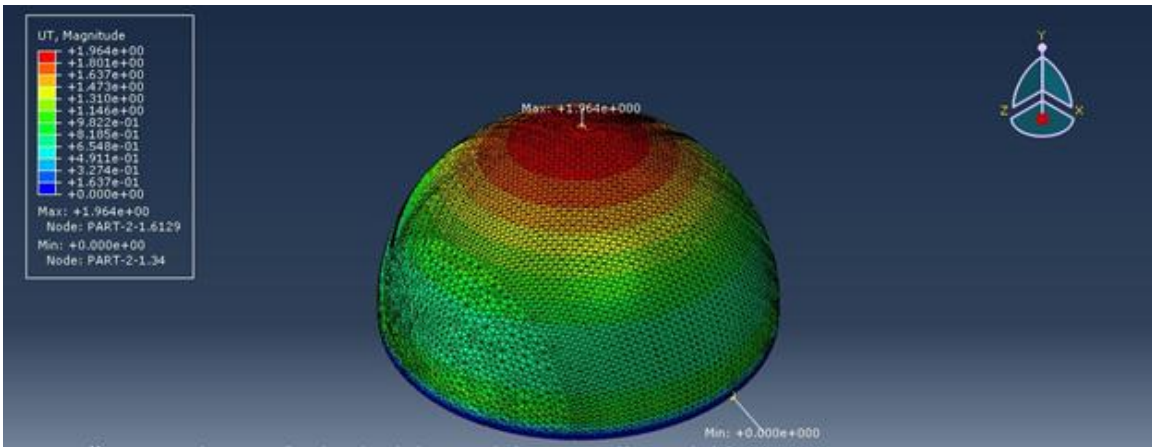


Figure 7 - Translation Distribution

3.2.6 Load Combinations

To apply the selected load case, the nature of the loading step was replaced with “Static; Linear Perturbation”. The self-weight was taken as the superimposed dead load, designated as “D”, and a factor of 1.2 was utilized. In contrast, 1.6 was the factor utilized for the roof load which was also selected from the ASCE 7-10 Manual Section 2.3. Figure 8 shows the stress response of the shell under this load combination, where the maximum stress was computed as 2709 psi which greater than the compressive strength of the concrete used which is 2500 psi. Figure 9 shows the maximum displacement which is 2.384 inches which

according to the thumb rule of ‘span length divided by 300’ [13] equals maximum allowable deflection, which implies that 2.384 inches is less than 7.1952 inches, therefore it is within the allowable range. However, to ensure that the structure is completely safe, we utilized the concrete damaged plasticity properties specified by Jankowiak and Lodygowski (2005) [12] as shown in Table 1.

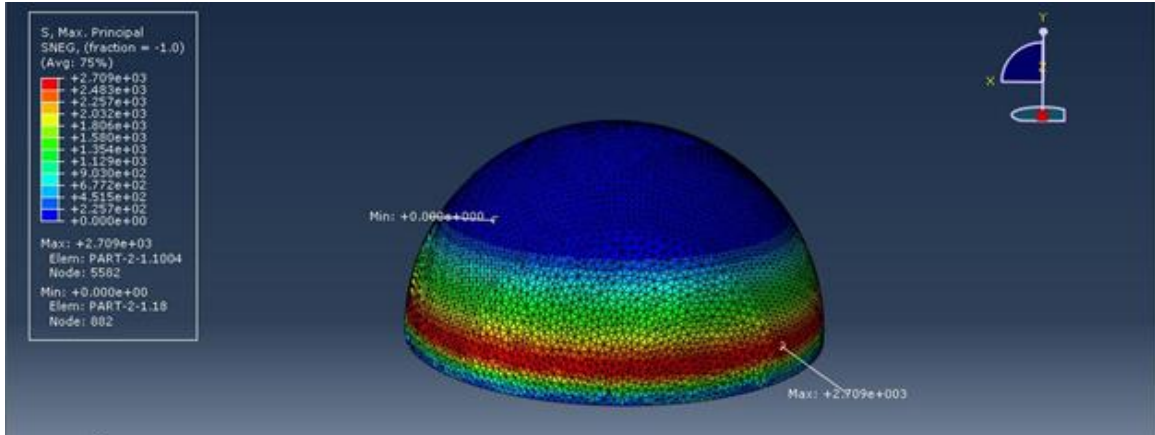


Figure 8 - Stress Distribution

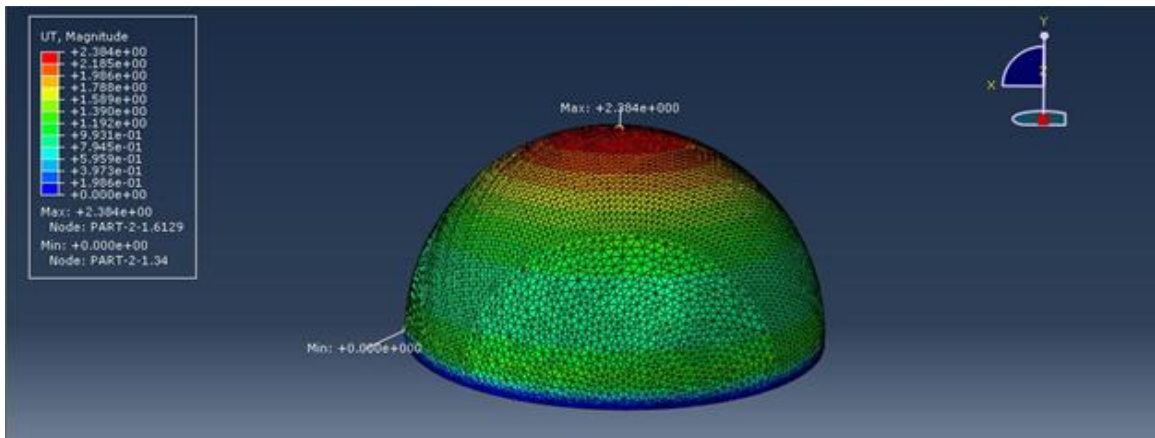


Figure 9 - Translation Distribution

Material's parameters	B50	The parameters of CDP model	
		β	38°
Concrete elasticity		m	1
E [GPa]	19.7	$f = f_{t0} / f_c$	1.12
ν	0.19	γ	0.666
Concrete compression hardening		Concrete compression damage	
Stress [MPa]	Crushing strain [-]	DamageC [-]	Crushing strain [-]
15.0	0.0	0.0	0.0
20.197804	0.0000747307	0.0	0.0000747307
30.000609	0.0000988479	0.0	0.0000988479
40.303781	0.000154123	0.0	0.000154123
50.007692	0.000761538	0.0	0.000761538
40.236090	0.002557559	0.195402	0.002557559
20.236090	0.005675431	0.596382	0.005675431
5.257557	0.011733119	0.894865	0.011733119
Concrete tension stiffening		Concrete tension damage	
Stress [MPa]	Cracking strain [-]	DamageT [-]	Cracking strain [-]
1.99893	0.0	0.0	0.0
2.842	0.00003333	0.0	0.00003333
1.86981	0.000160427	0.406411	0.000160427
0.862723	0.000279763	0.69638	0.000279763
0.226254	0.000684593	0.920389	0.000684593
0.056576	0.00108673	0.980093	0.00108673

Table 1 - Concrete Damaged Plasticity Module

The values for stress were converted from Pa to psi for coherency of units within the ABAQUS model. Figure 10 shows the stress response of the new model in which the maximum stress is 2709 psi and maximum displacement is 2.384 inches as shown in Figure 11.

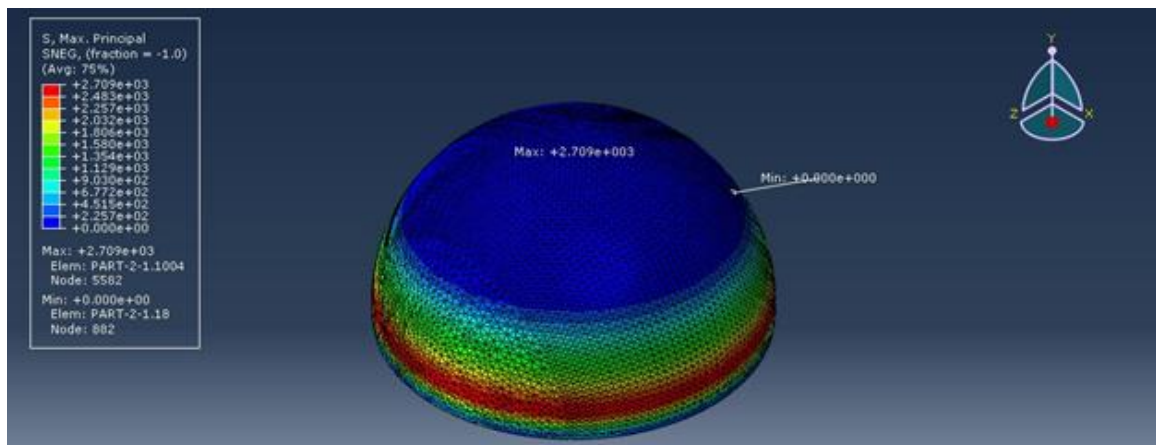


Figure 10 - Stress Distribution

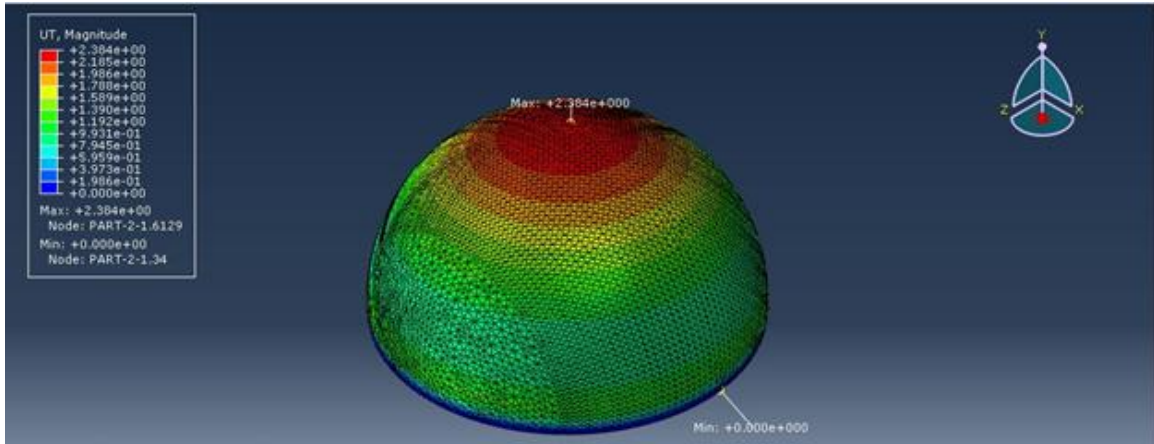


Figure 11 - Translation Distribution

3.2.7 Further Iterations

To tackle the problem of making the structure safe in lieu of the obvious failure in terms of stresses, the compressive strength of the concrete was increased to 3000 psi, which brought the Young's modulus of elasticity to 3122018.577 psi. Figure 12 shows that the maximum stress i.e. 2709 psi was less than the compressive strength of the concrete and Figure 13 shows that the maximum displacement which was reduced to 2.181 inches, therefore, making the structure safe under its self-weight and the designated roof load.

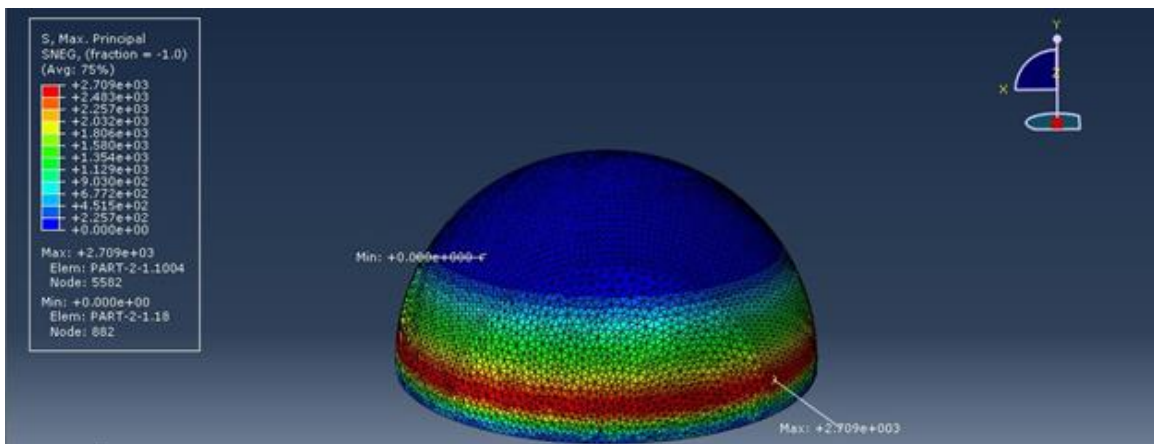


Figure 12 - Stress Distribution

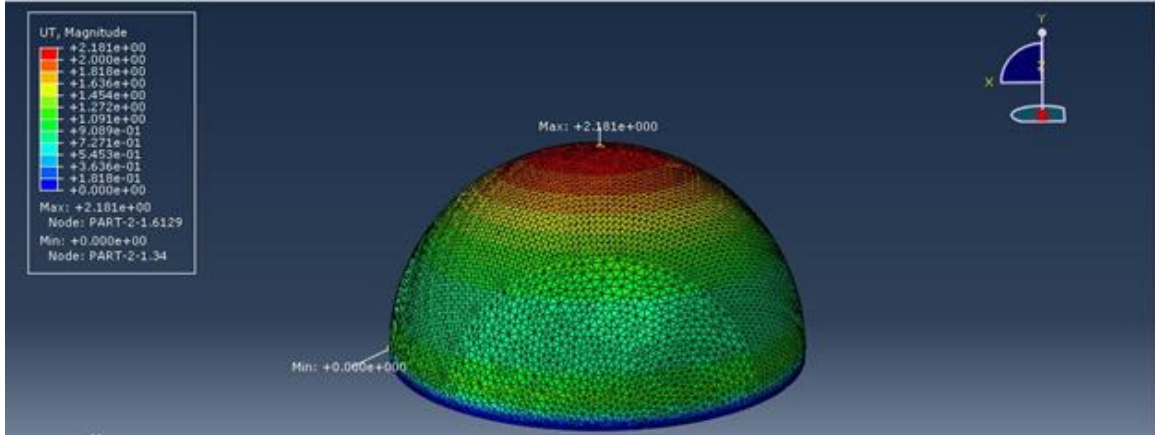


Figure 13 - Translation Distribution

3.3 Comparison with an Equivalent Frame Structure

In this section, the results obtained from the ABAQUS model were compared with results obtained from an equivalent frame. Here, equivalent means that both structures utilized similar amount of material and covered equal area. This was done to show that the shell structure is more stable and economical than the traditional block frame structures. The equivalent frame used was NUST's Jinnah Auditorium.

3.3.1 Code Selection

The software that was used to create the model of Jinnah Auditorium was CSI Etabs. Etabs was chosen over ABAQUS because of its specialization in modelling and analysis of 1:1 scale structure. The required architectural files were acquired from NUST's Project Management Office (PMO) in the form of AutoCAD drawing files.

The drawings were extensively studied and analysed to create a better understanding of the complex structure of Jinnah Auditorium.

Starting with the model on Etabs, the display units were selected as U.S. Customary since the AutoCAD drawings were in the same units. For design codes, AISC 360-10 was used

as the steel design where as ACI 318-14 was for Concrete design as shown in the Figure 14.

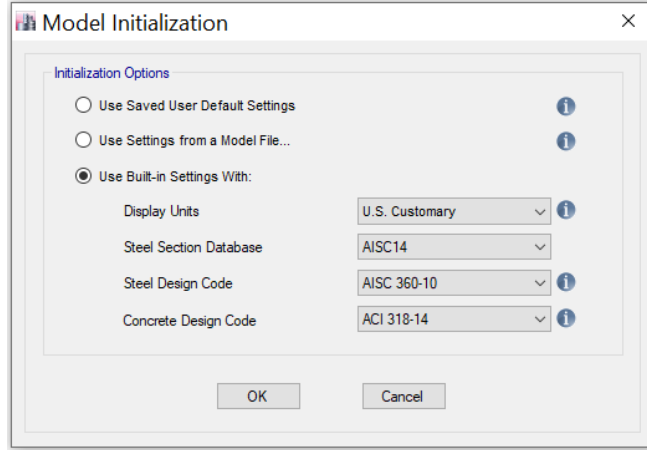


Figure 14 - Code Selection

3.3.2 Materials Definition

For selecting the material, PMO provided the strength of concrete used in the auditorium which are as follows:

Section	Grade of Concrete (psi)
Beam	3000
Column	3000
Slab	3000
Wall	3000
Dome	2400
Shell	2400

Table 2 - Concrete Strengths

For steel, as it was not provided by PMO, grade 60 was used because it is most used in constructions in Pakistan.

3.3.3 Members Definition

Cross-sections of all types of members were then defined in Etabs using the data provided in the architectural drawings.

There were 15 types of different column cross sections, some of them being different than the traditional circular, rectangular, and L-shaped sections, which required special design for them in the “Section designer” of Etabs. Reinforcement was provided in the cross section in accordance with the architectural drawings. And the “Reinforcement to be checked” option was selected rather than the “Reinforcement to be designed” as it was analysis of existing structure and not the design of a proposed one.

53 different types of beams were used in the auditorium. Each one of the cross-sections was defined in Etabs with the dimensions provided in the architectural drawings. Since there is not an option for just analysis of existing reinforcement for beams like that of columns, the beams reinforcements were set to be designed according to the loads applied later. Beams from B45 to B49 which are placed below the cantilever slab section of the first floor, were missing from the drawings provided by PMO. Therefore, assumed cross-sections of those beams were placed which were to be later modified if need be.

Slab thickness remained constant as 8” throughout all the floors, so only one cross-section of the slab was defined in Etabs. The middle of the roof was waffle slab so a new waffle cross-section specific to that part was also defined in accordance with the data provided in the drawings.

There are four different cross-sectional dimensions of shear wall provided in the auditorium. Each one of them was defined in Etabs for the model. Like the beams, there was not an option to specify the reinforcement to be analysed, rather the only option available was the reinforcement to be designed according to the load applied later.

3.3.4 Grid Layout and Members Placement

The grid was defined in two parts to cater for the part circular and part rectangular shape of the auditorium building. First the circular grid system was defined as shown in the Figure 15, with the radial distance between two grids as being the minimum radial distance between two columns in the columns layout plan of the architectural drawings. And the degree of the two grids were set as the minimum degrees available between two closest columns in the column layout drawing.

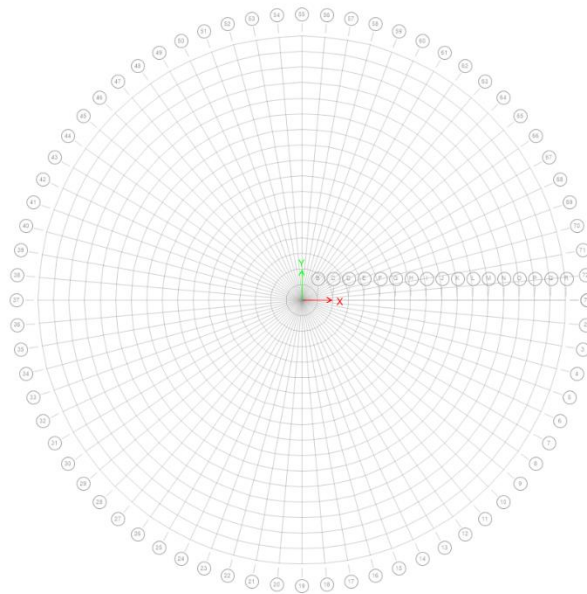


Figure 15 Circular Grid System

All the columns in the circular portion of the building was laid out before placing the rectangular grid system for the rectangular part of the building.

The columns were laid out by measuring from the architectural drawings, the distance between the specific column and the centre point of the circular portion of the building and then dividing that distance with the radial dimension of the grid to approximately finding one coordinate of the column on the Etabs grid system.

For the second coordinate, the degree of offset of the specific column in the architectural drawing was measured from the global x-axis of the drawing as reference point and then

the degree of offset was divided with the degrees of the grid system and therefore finding the approximate location of the column.

Once all the columns in the circular portion of the building were laid out, a new rectangular grid system was created as shown in the Figure 16, with calculating the offset required from the centre of the circular grid system and similar to the previous method, measuring the distance between the two nearest columns in the columns layout plan, and accordingly setting the dimension of each grid in the new grid system.

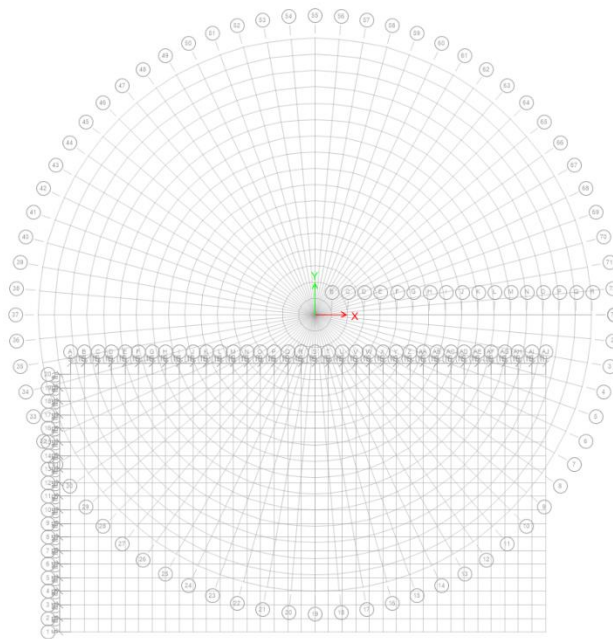


Figure 16 - Circular & Rectangular Grids in Combination

For placing the remaining columns, already placed columns on the edge of the circular portion were used as reference and distance between those columns on the edge to the specific column to be placed was measured and then the distance was divided with dimension of the grid to find the approximate location of the column.

Since the rectangular portion of the building is not perfectly rectangular and has curvature in it as well. The offset of the curvature was calculated by using the hypotenuse of the two columns in the curvature from the drawings to find the appropriate components of x and y

axis and approximately placing the columns in the rectangular grid system to form the curvature of the building.

The length of the shear walls was measured from the architectural plans and then by dividing the length with the minimum dimension of the radial grid, approximate length on the grid system was calculated. The shear walls were placed using the “Draw Walls” command and then selecting the required shear wall to be placed.

Once all the columns and shear walls of the ground floor were placed as shown in the Figure 17, respective beams were placed between the respective columns as shown in the Figure 18, using the beam layout plan of the drawings.

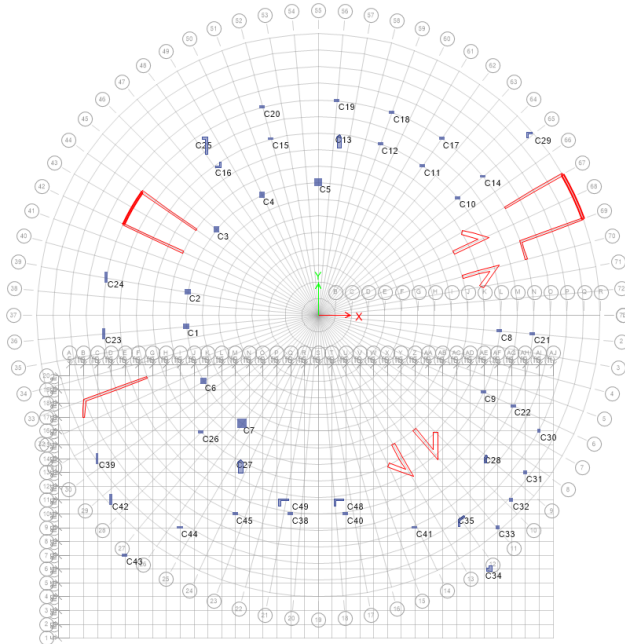


Figure 17 - Columns & Shear Walls Placed on Grid

Most of the beams in the building are curved, so the “3 points arc” was used provide the required curvature in the beams.

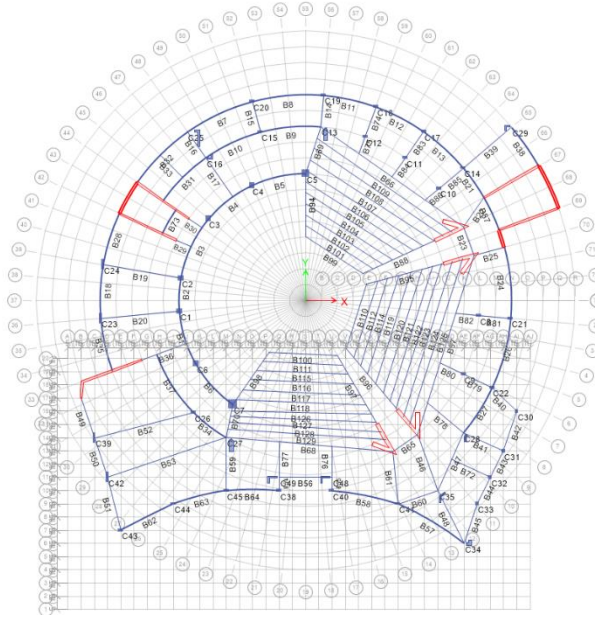


Figure 18 - Beams Placed

Once all the beams of the ground floor were placed, the slab was placed over them. Since two dimensions of slab were straight lines while the other two were curved, mixture of the “straight line” command and “3 points arc” command was used while placing the slabs over the beams.

The height of the first floor and roof was taken 18 feet and 21 feet respectively from the front view in the architectural plans.

Once the ground floor was completed, the same columns and shear walls were placed on the first floor over the top of the already existing ones in the ground floor as all columns and shear walls extend till the roof in the plans provided by PMO.

Like the ground floor, all the beams were placed according to the first-floor beams plan, the curved beams were curved using the same tool “3 points arc”.

Once all the slabs sections were placed on top of the first floor in similar fashion to that of the ground floor, the waffled slab section was placed on the middle part of the roof where large span of length was needed without provision of any vertical support as shown in the Figure 19. The frame structure was now complete.

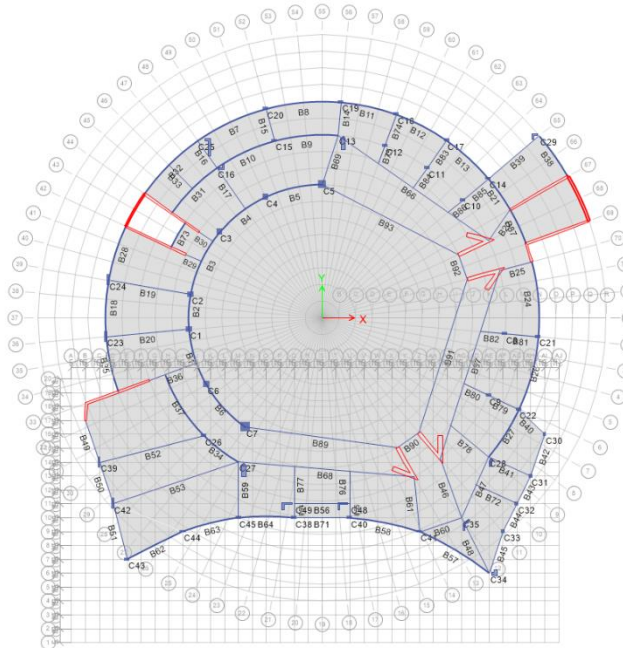


Figure 19 - Completed Frame Structure

The base supports were changed from “pin” to “fix” support and the connection between all the members were made “continuous” as well.

3.3.5 Check on Model

The model was then checked for any connection errors by going into the “Check Model” option. All the errors were resolved by just placing the faulty members again in the same manners.

3.3.6 Applied Loads and Load Combinations

Loads were then applied by taking the dead load as self-load of the structure and live load as 100 psf on the first floor and 20 psf on roof which were consulted by the ASCE 7-10. And the load combination was used as $1.2D + 1.6L + 0.5L_r$ referred from ACI 318-19 as show in the table 3.

Load combination	Equation	Primary load
$U = 1.4D$	(5.3.1a)	D
$U = 1.2D + 1.6L + 0.5(L_r \text{ or } S \text{ or } R)$	(5.3.1b)	L
$U = 1.2D + 1.6(L_r \text{ or } S \text{ or } R) + (1.0L \text{ or } 0.5W)$	(5.3.1c)	$L_r \text{ or } S \text{ or } R$
$U = 1.2D + 1.0W + 1.0L + 0.5(L_r \text{ or } S \text{ or } R)$	(5.3.1d)	W
$U = 1.2D + 1.0E + 1.0L + 0.2S$	(5.3.1e)	E
$U = 0.9D + 1.0W$	(5.3.1f)	W
$U = 0.9D + 1.0E$	(5.3.1g)	E

Table 3 - Load Combinations

3.3.7 Meshing and Analysis

Meshing for the slabs was kept to default and the structure was ran for analysis. After the analysis was completed, concrete design check was applied. When the processing completed, Etabs showed which members could possibly fail under the current loading. The failed members were checked for the cause of failure by going into the summary of the report. Since the members failed because of the exceeded torsion capacity, those members were then freed of the torsion end restriction.

3.3.8 Stress Distribution and Deformations

The deformed shape of the structure as shown in the Figure 20, was analysed for maximum deflection (see Appendix A) which came out to be 0.009941 inches.

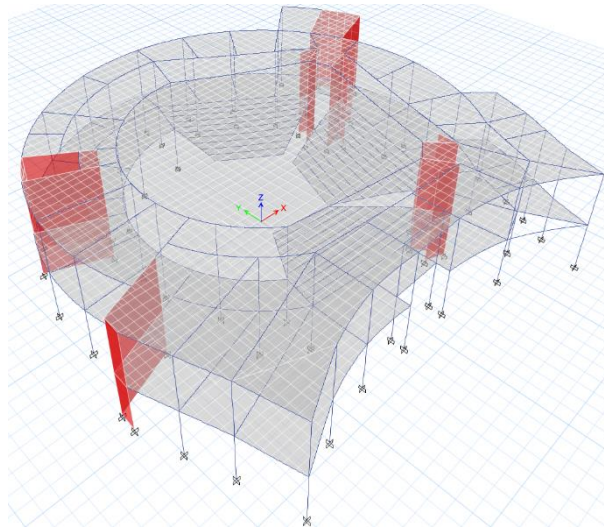


Figure 20 - Deformed Structure

The stress distribution on the model as shown in the Figure 21 was analysed for points of maximum stress which came out to be 30033.03 psi.

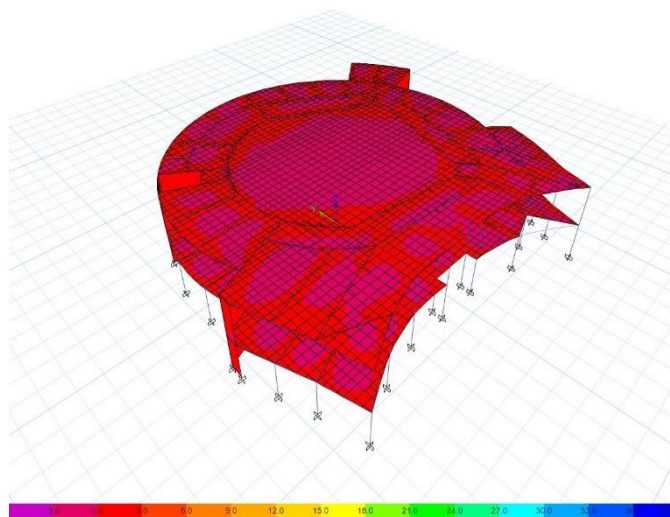


Figure 21 Stress Distribution

And then the total volume of concrete and weight of reinforcement was calculated which came out to be 57453.31 ft³ and 122.626 tonnes, respectively.

3.4 Provision for Stability of Shell Formwork

As discussed in section 3.1, the core focus of this project was to propose a semi-spherical hollow dome that was not only easy to construct but at the same time served as an optimized solution for moving away from the undesired block-shaped reinforced concrete frame structures that are ubiquitous in Pakistan. For simplicity and to establish grounds for further research, this study limited its scope to proposing an alternative dome to large block shaped structures prevalent in Pakistan that are used to cover long spans.

To supplement the efforts for the achievement of the aforementioned objectives, a small model was prepared which draws attention to how an average shell structure, which is under construction or hasn't yet achieved its design strength, is made stable with the help of scaffoldings and props. The model helps in visualizing how the temporary works help keep the shell structure stable and withstand loads when its own strength has not yet developed.

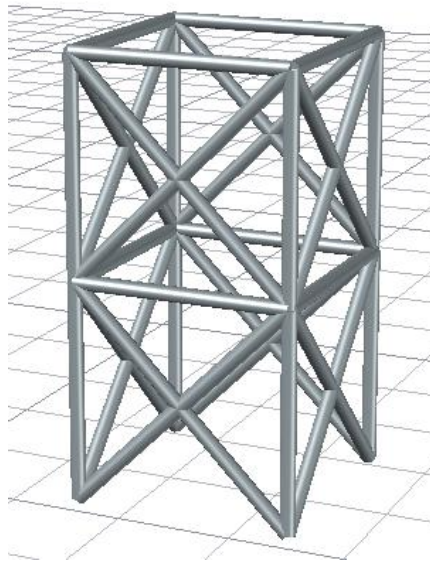


Figure 22 Strengthened Temporary Work frame (Type A)

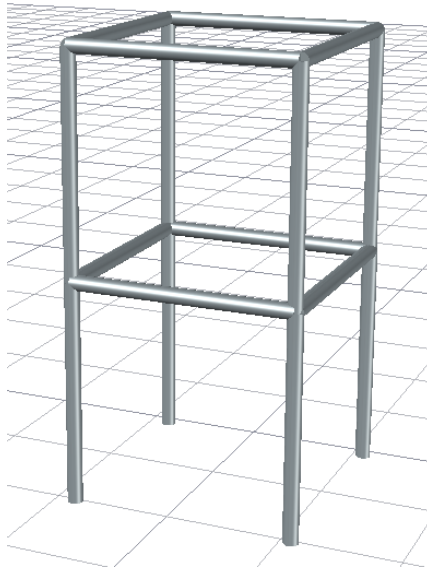


Figure 23 Non-strengthened Temporary Work Frame (Type B)

Figure 23 shows a portion of the temporary works frame which has been strengthened by diagonal bracings. Similarly, Figure 24 shows the portion of temporary works frame which is unbraced. Both figures show the arrangement of type 4 steel tubes (BS EN 39:2001, the most common type of steel tubes used in scaffoldings) which, when part of a temporary works frame structure, would keep a shell structure, similar to the one used in section 3.2, stable and help it resist the usual loads. The vertical steel tubes help resist the vertical loads. Similarly, the diagonal arrangement of steel tubes helps in countering the lateral forces due to wind, on-site vibrations, moving workers, and machinery.

The black squares in Figure 25 show the positioning of Type-A frames in the temporary works framing of a dome type shell structure like the one discussed in section 3.1. This arrangement of strengthened frames will keep the dome above it stable against both vertical and lateral forces. In Figure 25, the thin circles, and the spaces between them represent the places along which Type-B frames will be placed. Type-B frames will be joined with each other (see Appendix B) and with the adjoining Type-A frames, just like in a regular rectangular temporary works framing.

Such an arrangement of temporary works, and its variations, can be used to successfully support a shell structure of any shape and size.

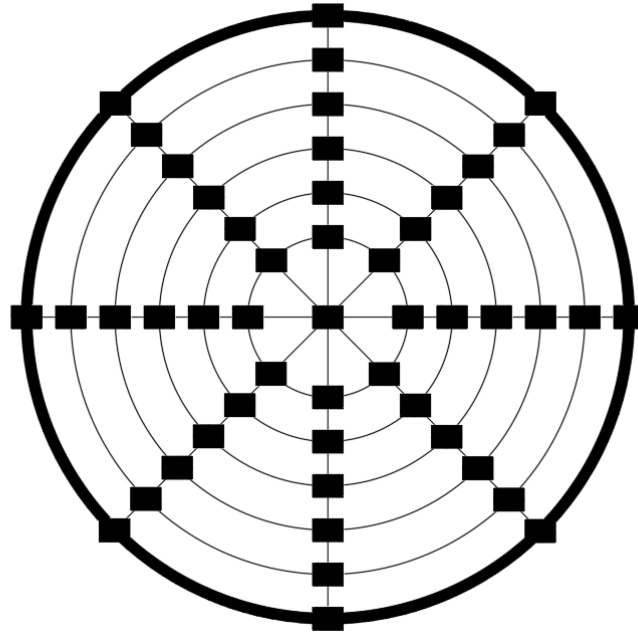


Figure 24 Arrangement of Type-A frame in a Dome Temporary Works

RESULTS

Following are the tables which summarize the important results obtained from both the models:

4.1 Parameters from ETABS

PARAMETERS	VALES
Maximum Stress (psi)	30033.03
Maximum Displacement (in)	0.0099
Volume Concrete (cft)	57453.31
Theoretical Weight of Steel (tons)	122.63

Table 4 - Parameters for ETABS Model

1. Cost of Concrete = 12171483.13 PKR
2. Cost of Steel = 13112825.90 PKR

4.2 Parameters from ABAQUS

PARAMETERS	VALES
Maximum Stress (psi)	2709
Maximum Displacement (in)	2.181
Volume Concrete (cft)	25271
Theoretical Weight of Steel (tons)	53.94

Table 5 - Parameters for ABAQUS Model

1. Cost of Concrete = 5353661.35 PKR
2. Cost of Steel = 5768084.20 PKR

4.3 Comments

The structures on ABAQUS and ETABS were analyzed to ascertain the maximum stress and displacement to compare their performance under the selected load cases.

The quantities of the steel and concrete in the actual auditorium building were calculated and were used to compute the concrete to steel ratio. The values were then used to calculate the theoretical amount of steel that would be utilized in the construction of the proposed shell structure.

Subsequently, the market rate system published by the Government of Punjab in 2016, which is when it was last updated, was used to extract the rates of a standard reinforced concrete (1:2:4) whose rate was 211.85 PKR per cubic feet. The rate of steel was 5346.76 PKR per hundred pounds. The total volume of concrete and weight of steel were multiplied with their respective rates to compute the final cost, which encompassed labor costs, manufacturing, procurement, and logistics.

CONCLUSIONS

From Table 4 and Table 5, it can be ascertained that the shell structure designed on ABAQUS performs significantly better under the assigned load cases in contrast to the selected auditorium's structural performance as determined via ETABS. The structural performance of the shell enables it to distribute stresses uniformly across structure. The structure is less complex and easy to construct considering the formwork.

Additionally, a cost analysis of the two structures, indicates that constructing the shell will yield a 56% reduction in construction costs.

This indicates that the designed shell structure is structurally efficient, with the added benefit of being cost efficient.

CHAPTER 6

RECOMMENDATIONS

One key aspect of this project which was hoped to be achieved was successfully executing shape optimization of the design shell structure, to minimize stresses and strains across the shell whilst maintaining the same amount of concrete. Considering the pandemic which has engulfed the globe and affected day-to-day workings of academic institutions coupled with lack of processing power and time, have hindered our ability to achieve this goal. Initial and more simplistic iterations involved freezing boundary conditions and executing the optimization module, which would in turn lead to the optimization job being aborted early in the optimization cycle. The error message would indicate that the design nodes were restricted from moving out of place to produce the optimum shape which minimized stresses and strains across the structure. It is recommended that further research be done to tackle this issue.

APPENDICES

APPENDIX A

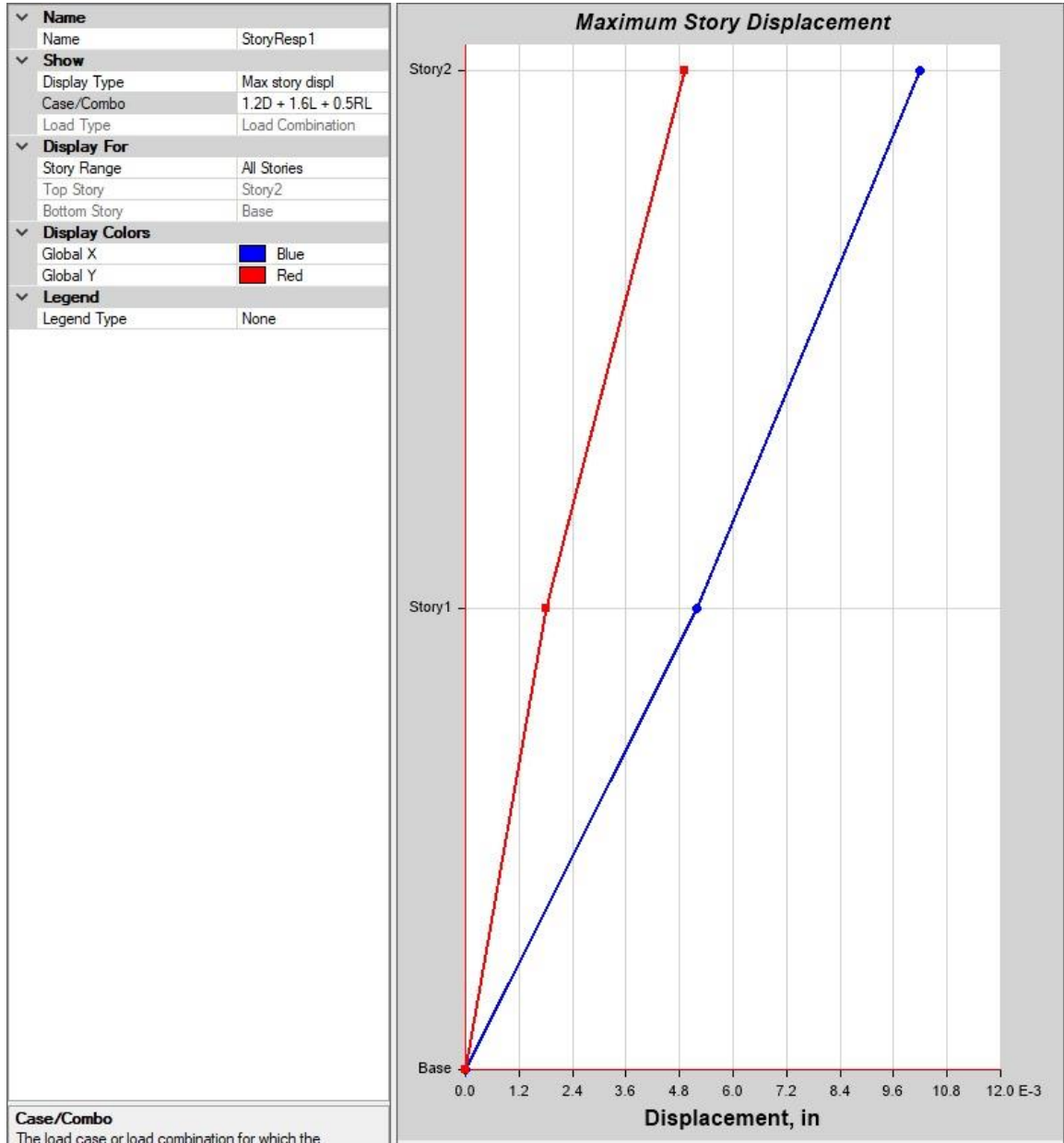


Figure 25 Maximum story displacements of ETABS model

APPENDIX B

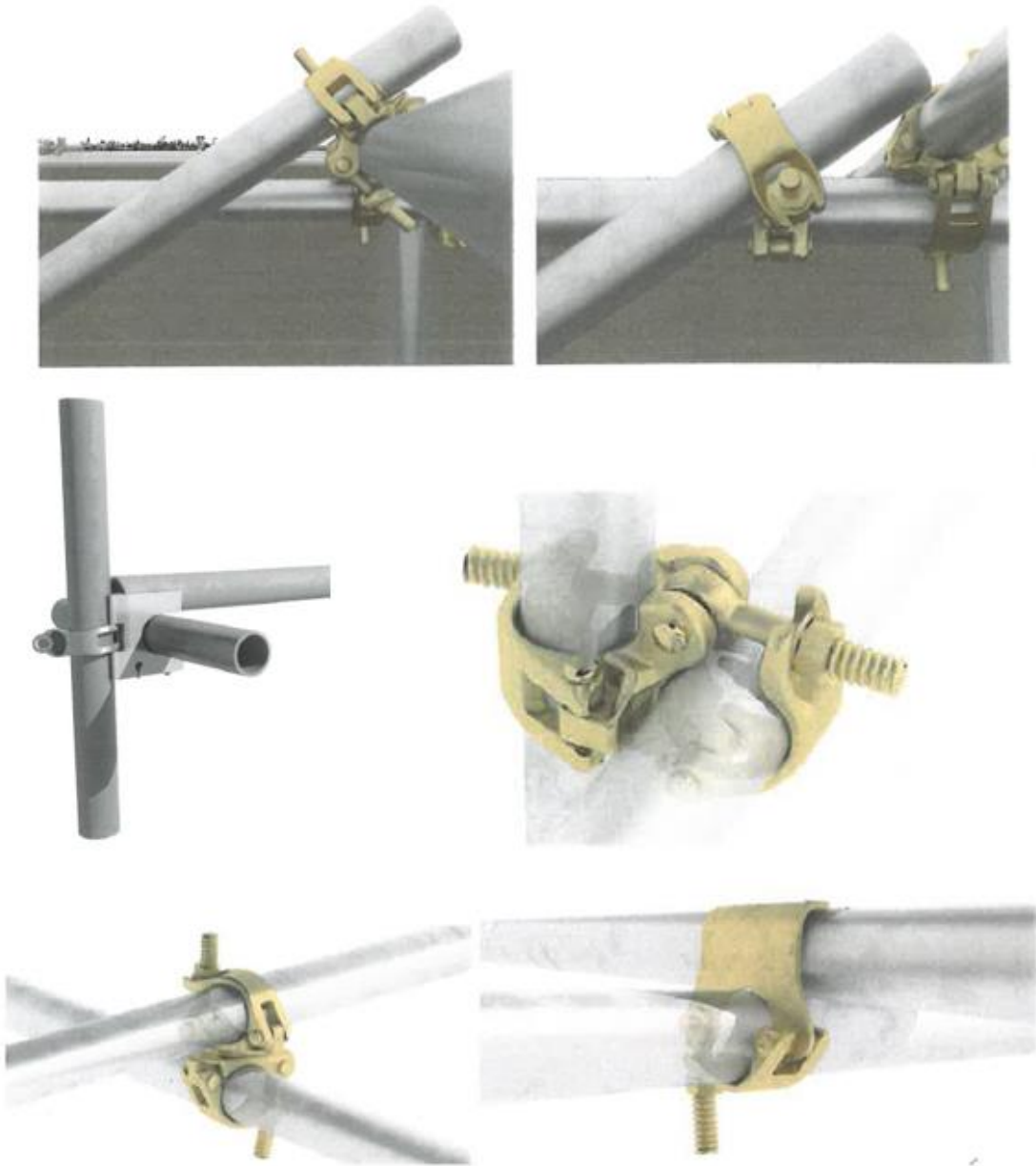


Figure 26 Different types of joints used in steel tube temporary works

REFERENCES

- [1] Ohmori H, Yamamoto K. Shape optimization of shell and spatial structures for specified stress distribution - Part 1: Shell analysis. *J IASS* 1998;39(126):3_13
- [2] Bletzinger, K.U. and Ramm, E. (1993), "Form finding of shells by structural optimization", *Engineering with Computers*, Vol 9, pp. 27-35.
- [3] Rao, N.V.R. and Hinton, E. (1993), "Structural optimization of variable thickness plates and free form shells", *Structural Engineering Review*, Vol 5, pp. 1-21.
- [4] Afonso, S.M.B. and Hinton, E. (1995), "Free vibration analysis and shape optimization of variable thickness plates and shells-II, sensitivity analysis and shape optimization", *Structural Engineering Review*, Vol. 10, pp. 47-66.
- [5] Ghasemi, M. R. (1996), "Structural Optimization of Trusses and Axisymmetric Shells Using Gradient-Based Methods and Genetic Algorithm", Ph.D. thesis, University of Wales, Swansea, UK.
- [6] Lee, S.J. (1998), Analysis and optimization of shells, Ph.D. Thesis, Dept. of Civil Eng., Univ. Col... of Swansea.
- [7] Hinton, E. Ozakca, M. and Rao N.V.R. (1995), "Free vibration analysis and shape optimisation of variable thickness prismatic folded plates and curved shells, Part 1 and 2", *J. Sound and Vibration*, Vol 181, pp.567-581.
- [8] Rao, N.V.R., and Hinton, E. (1994), "Analysis and optimisation of prismatic plate and shell structures with curved planform, Part 2 --- shape optimisation", *Computers and Structures*, Vol. 52, pp. 341-351.
- [9] Shimoda M., Ikeya K. (2019) Free-Form Optimization of a Shell Structure with Curvature Constraint. In: Andrés-Pérez E., González L., Periaux J., Gauger N., Quagliarella D., Giannakoglou K. (eds) *Evolutionary and Deterministic Methods for Design Optimization and Control with Applications to Industrial and Societal Problems. Computational Methods in Applied Sciences*, vol 49. Springer, Cham
- [10] Fujita S., Ohsaki M. (2010) Shape Optimization of Free-form Shells Using Invariants of Parametric Surface. In: *International Journal of Space Structures* Vol. 25 No. 3 2010
- [11] Gotsis P. K. (1994) Structural Optimization of Shell Structures. In: *Computers & Structures* Vol. 50, No. 4. pp. 499-507, 1994, Elsevier Science Ltd.

[12] Jankowiak T., Lodygowski T. (2005). Identification of Parameters of Concrete Damage Plasticity Constitutive Model. From Institute of Structural Engineering, Poznan University of Technology.

[13] Orton A. The Way We Build Now: Form, Scale and Technique. Spon, 1990